Observation and Spectroscopy of New Proton-Unbound Isotopes ^{30}Ar and ^{29}Cl: An Interplay of Prompt Two-Proton and Sequential Decay

I. Mukha,[1,2] L. V. Grigorenko,[3,4,2] X. Xu,[5,1,6] L. Acosta,[7,8] E. Casarejos,[9] A. A. Ciemny,[10] W. Dominik,[10] J. Duénas-Díaz,[11] V. Dunin,[12] J. M. Espino,[13] A. Estradé,[14] F. Farinon,[1] A. Fomichev,[3] H. Geissel,[1,5] T. A. Golubkova,[15] A. Gorshkov,[3] Z. Janas,[10] G. Kamiński,[16,3] O. Kiselev,[1] R. Knöbel,[1,5] S. Krupko,[3] M. Kuich,[17,10] Yu. A. Litvinov,[1] G. Marquinez-Durán,[11] I. Martel,[11] C. Mazzocchi,[10] C. Nociforo,[1] A. K. Ordúz,[11] M. Pfützner,[10,1] S. Pietri,[1] M. Pomorski,[10] A. Prochazka,[1] S. Rymzhanova,[3] A. M. Sánchez-Benítez,[11] C. Scheidenberger,[1,5] P. Sharov,[3] H. Simon,[1] B. Sitar,[18] R. Slepnev,[3] M. Stanoiu,[19] P. Strmen,[18] I. Szarka,[18] M. Takechi,[1] Y. K. Tanaka,[1,20] H. Weick,[1] M. Winkler,[1] J. S. Winfield,[1] and M. V. Zhukov[21]

[1]*GSI Helmholtzzentrum für Schwerionenforschung, 64291 Darmstadt, Germany*
[2]*National Research Centre "Kurchatov Institute," Kurchatov square 1, 123182 Moscow, Russia*
[3]*Flerov Laboratory of Nuclear Reactions, JINR, 141980 Dubna, Russia*
[4]*National Research Nuclear University "MEPhI," 115409 Moscow, Russia*
[5]*II.Physikalisches Institut, Justus-Liebig-Universität, 35392 Gießen, Germany*
[6]*School of Physics and Nuclear Energy Engineering, Beihang University, 100191 Beijing, China*
[7]*INFN, Laboratori Nazionali del Sud, Via S. Sofía, 95123 Catania, Italy*
[8]*Instituto de Física, Universidad Nacional Autónoma de México, México, D.F. 01000, Mexico*
[9]*University of Vigo, 36310 Vigo, Spain*
[10]*Faculty of Physics, University of Warsaw, 02-093 Warszawa, Poland*
[11]*Department of Applied Physics, University of Huelva, 21071 Huelva, Spain*
[12]*Veksler and Baldin Laboratory of High Energy Physics, JINR, 141980 Dubna, Russia*
[13]*Department of Atomic, Molecular and Nuclear Physics, University of Seville, 41012 Seville, Spain*
[14]*University of Edinburgh, EH1 1HT Edinburgh, United Kingdom*
[15]*Advanced Educational and Scientific Center, Moscow State University, 121357 Moscow, Russia*
[16]*Institute of Nuclear Physics PAN, 31-342 Kraków, Poland*
[17]*Faculty of Physics, Warsaw University of Technology, 00-662 Warszawa, Poland*
[18]*Faculty of Mathematics and Physics, Comenius University, 84248 Bratislava, Slovakia*
[19]*IFIN-HH, Post Office Box MG-6, Bucharest, Romania*
[20]*University of Tokyo, 113-0033 Tokyo, Japan*
[21]*Fundamental Physics, Chalmers University of Technology, S-41296 Göteborg, Sweden*

(Received 6 August 2015; published 9 November 2015)

Previously unknown isotopes ^{30}Ar and ^{29}Cl have been identified by measurement of the trajectories of their in-flight decay products $^{28}\mathrm{S}+p+p$ and $^{28}\mathrm{S}+p$, respectively. The analysis of angular correlations of the fragments provided information on decay energies and the structure of the parent states. The ground states of ^{30}Ar and ^{29}Cl were found at $2.25^{+0.15}_{-0.10}$ and 1.8 ± 0.1 MeV above the two- and one-proton thresholds, respectively. The lowest states in ^{30}Ar and ^{29}Cl point to a violation of isobaric symmetry in the structure of these unbound nuclei. The two-proton decay has been identified in a transition region between simultaneous two-proton and sequential proton emissions from the ^{30}Ar ground state, which is characterized by an interplay of three-body and two-body decay mechanisms. The first hint of a fine structure of the two-proton decay of $^{30}\mathrm{Ar}^{*}(2^{+})$ has been obtained by detecting two decay branches into the ground and first-excited states of the ^{28}S fragment.

DOI: 10.1103/PhysRevLett.115.202501 PACS numbers: 23.50.+z, 25.10.+s, 27.20.+n

Nuclei beyond the proton drip line have been intensively investigated in recent years, because they exhibit exotic new phenomena that cannot be found in stable nuclei. For instance, two-proton ($2p$) radioactivity was discovered [1,2]. This phenomenon, predicted by Goldansky in 1960 [3], manifests a complicated few-body dynamics of "true $2p$" (or "true three-body") decays. Because of the pairing effect in nuclei, the sequential emission of protons from the true-$2p$ precursors is not possible, which forces simultaneous (i.e., prompt) emission. As a result, three-body effects lead to extremely long half-lives of true-$2p$ precursors and specific correlations of their fragments [4]. Besides making further observations of $2p$ radioactivity in ^{54}Zn and ^{48}Ni [5,6], a study of p-p correlations for the p-f-shell $2p$ precursor ^{45}Fe has been performed [7]. Similar correlation studies were also attempted for ^{54}Zn and ^{48}Ni

[8,9], but due to very small statistics no conclusions on the decay mechanism could be drawn. The three-body decay mechanisms of short-living "democratic" $2p$ emitters ^{6}Be and ^{16}Ne were studied in broad energy ranges [10–12]. The first case of $2p$ radioactivity in an s-d shell was found in the ^{19}Mg isotope by measuring its decay in flight with a novel tracking technique [13]. In spite of the experimental advances, most $2p$-decay precursors remain unexploited.

In this Letter, we report on the discovery and spectroscopic study of the $2p$ emitter ^{30}Ar and its neighbor ^{29}Cl. The experiment is based on in-flight decay of the $2p$ emitters and the tracking of the decay-product trajectories by microstrip silicon detectors. Previous applications of this method can be found in Refs. [13–17].

Experiment.—Secondary ^{31}Ar ions were produced in the fragment separator (FRS) [18] by fragmenting an 885 AMeV ^{36}Ar primary beam accelerated by the SIS facility at GSI (Darmstadt, Germany) in an 8 g/cm^2 ^{9}Be target. To separate the ^{31}Ar fragments, a 5-g/cm^2-thick aluminum wedge degrader was installed at the first focal plane of the FRS. The wedge was shaped for an achromatic focusing of the 620 AMeV ^{31}Ar beam on the secondary 4.8-g/cm^2-thick ^{9}Be target located at the midplane of the FRS. The ^{31}Ar intensity was about 50 ions s^{-1}, and ^{30}Ar ions were produced via one-neutron knockout reactions in the secondary target. A set of four large-area microstrip silicon detectors was positioned downstream of the target to measure positions of all ^{30}Ar in-flight decay products, e.g., coincident two protons and a heavy-ion (HI) recoil. In addition, an optical time-projection chamber (OTPC) was used in the same experiment to observe beta decays of stopped ^{31}Ar ions, which passed the secondary target intact. With this detector, β-delayed $3p$ emission from ^{31}Ar was observed [19]. The experimental layout is sketched in Fig. 1.

The detector setup around the secondary target allowed a reconstruction of all fragment and decay-product trajectories, angles, and the position of the corresponding decay vertex. Angular $\theta(p\text{-}p)$ and $\theta(\text{HI-}p)$ correlations were obtained with a resolution of 1 mrad. The uncertainty of the $2p$-precursor half-life, derived from the uncertainty of the measured center of gravity of the decay-vertex distribution [13], was 3–5 ps. As was shown in Ref. [16] for the known states in ^{15}F, ^{16}Ne, and ^{19}Na, the identification of $2p$-precursor states as well as their decay energies and widths can be determined by analyzing the angular correlations of the decay products.

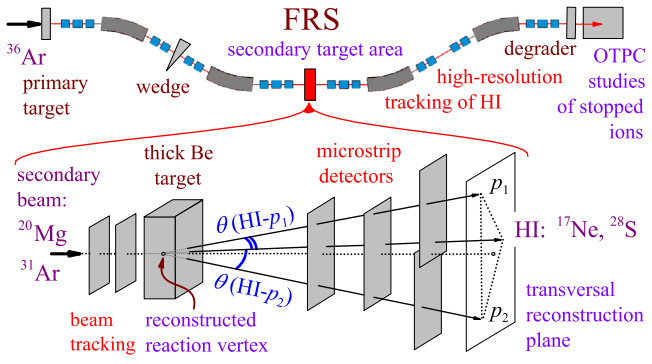

FIG. 1 (color online). Upper part: The experiment layout at the FRS fragment separator. Lower part: Sketch of the detector setup at the secondary-target area measuring trajectories of the incoming ^{31}Ar (^{20}Mg) ions and their decay products ^{28}S (^{17}Ne) and protons p_1 and p_2.

Reference case of ^{19}Mg.—The well-known $2p$ decay of ^{19}Mg was remeasured to determine angular and half-life ($T_{1/2}$) resolutions as well as the detection efficiency. The excitation spectrum of ^{19}Mg obtained as a function of angular $\theta(\text{HI-}p)$ correlations,

$$\rho_\theta = \sqrt{\theta^2(\text{HI-}p_1) + \theta^2(\text{HI-}p_2)},$$

has confirmed the peaks related to ^{19}Mg resonances with the total $2p$-decay energy $E_{2p} \sim \rho_\theta^2$ [16,17]. The observed peaks at 0.85(12), 2.1(3), and 5.3(4) MeV are consistent with the previous measurements [17]. The half-life $T_{1/2}$ of the ^{19}Mg ground state (g.s.) is measured as an upper limit $T_{1/2} < 10$ ps, which does not contradict the literature value of 4.0(15) ps [13]. Recently, the ^{19}Mg half-life was remeasured by another method as 1.2–4.4 ps [20].

Observation of ^{30}Ar *and* ^{29}Cl.—Figures 2(a) and 2(b) show the vertex profiles obtained from the $^{28}\text{S} + p + p$ events gated by the assumed ^{30}Ar "excited-state" and "ground-state" conditions, respectively. These gates are inferred from the respective angular ρ_θ correlations as discussed below in the context of Fig. 2(c). The Monte Carlo simulations [13,21] shown in Fig. 2(a) assume $T_{1/2} = 0$ for the ^{30}Ar states and take into account the above-mentioned experimental angular uncertainties in tracking the fragments in reconstructing the vertex coordinates. The simulations reproduce the data quantitatively. The half-life uncertainty is illustrated by the $T_{1/2} = 5$ ps simulation, which fails to fit the data. The asymmetry of the rising and falling slopes of the vertices is due to multiple scattering of the fragments in the thick target. This vertex profile serves as the reference for estimating the half-life of the ^{30}Ar g.s. Similar Monte Carlo simulations with $T_{1/2} = 0$ and $T_{1/2} = 10$ ps of the ^{30}Ar g.s. are compared with the corresponding data in Fig. 2(b). One may see that the $T_{1/2} = 0$ simulation is the best data fit, while the $T_{1/2} = 10$ ps calculation serves for illustration purpose. Thus, the half-life of the ^{30}Ar g.s. is shorter than 10 ps, which we assume as the upper limit.

The angular distribution ρ_θ of the measured $^{28}\text{S} + p + p$ events is shown in Fig. 2(c). Several peaks, labeled $A - H$, can tentatively be assigned to states in ^{30}Ar. Most of them are expected to emit protons sequentially via levels in the

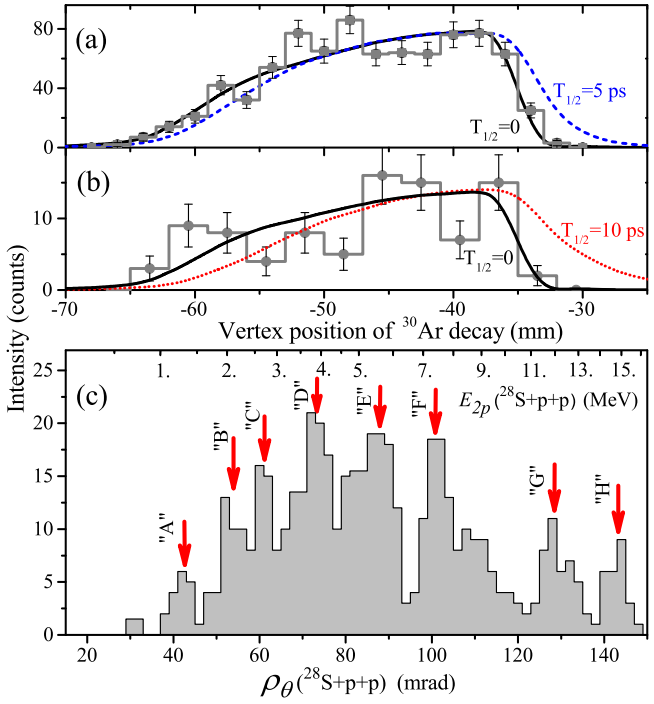

FIG. 2 (color online). (a),(b) Profiles of the $^{30}\mathrm{Ar} \rightarrow {}^{28}\mathrm{S} + p + p$ decay vertices along the beam direction with respect to the closest microstrip detector (histograms with statistical uncertainties). (a) The data gated by large angles $\rho_\theta > 60$ mrad, which corresponds to short-lived excited states in ^{30}Ar. (b) The data gated by $45 < \rho_\theta < 55$ mrad where the ground state of ^{30}Ar is expected. Solid, dashed, and dotted curves show the Monte Carlo simulations of the detector response for the ^{30}Ar $2p$ decays with half-life $T_{1/2}$ of 0, 5, and 10 ps, respectively. (c) Angular correlations ρ_θ of the measured $^{28}\mathrm{S} + p + p$ coincidences (filled histogram), which reflect the excitation spectrum of ^{30}Ar. The peaks "A"–"H" suggest ^{30}Ar states whose $2p$-decay energies are shown in the upper axis.

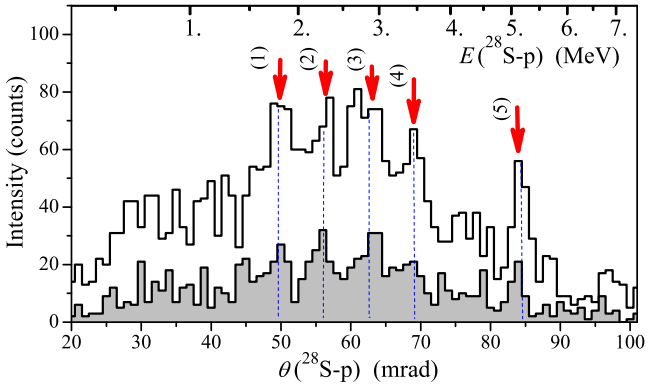

FIG. 3 (color online). Angular $\theta(^{28}\mathrm{S}\text{-}p)$ correlation derived from the measured $p + {}^{28}$S coincidences (the unfilled histogram). The suggested ^{29}Cl resonances (1–5) are indicated by arrows, and the respective $1p$-decay energies are given by the upper axis. The gray-filled histogram shows the similar correlation deduced from the $^{28}\mathrm{S} + p + p$ triple coincidences.

previously unknown isotope ^{29}Cl. Thus, we first derive the ^{29}Cl states on the basis of the measured $^{28}\mathrm{S} + p$ coincidences. Angular correlations $\theta(^{28}\mathrm{S}\text{-}p)$ obtained from the measured $p + {}^{28}$S and $^{28}\mathrm{S} + p + p$ coincidences give the peaks (1–5) in Fig. 3. In the former case, parent ^{29}Cl states may be populated via several possible reactions on ^{31}Ar, while the latter distribution is presumably due to the $2p$ emission from ^{30}Ar states.

Assignments of ^{29}Cl *states.*—The isobaric symmetry of mirror nuclei is used for assigning the ^{29}Cl states. The ^{29}Mg g.s. with spin parity $3/2^+$, which is a mirror of ^{29}Cl, is separated merely by 55 keV from the first excited state $1/2^+$; see Ref. [22]. By assuming a single-particle structure of ^{29}Mg, we infer the spectrum of ^{29}Cl in a two-body potential cluster model $^{28}\mathrm{S} + p$. The Coulomb displacement energy is evaluated with the charge radius of ^{28}S of 3.21(7) fm derived from systematics of the known isotopes ^{32,34,36}S [23]. The spin-orbit parameter for the potential model is defined by the spin parity $5/2^+$ of the 1.638 MeV state in ^{29}Mg. The calculated low-lying levels in ^{29}Cl are displaced in comparison to its isobaric mirror ^{29}Mg due to a strong Thomas-Ehrman shift (TES). The TES is an effect of the violation of the fundamental isobaric symmetry in the nuclear structure, which was introduced for single-particle states of sd-shell nuclei; see Refs. [24,25]. As the s and d orbitals have different radial extents, the energies of the respective isobaric-mirror states are different due to the Coulomb interaction. This provides a simple way for estimates of dominant orbitals. Studies of the TES were recently extended to nuclei with an even number of "valence" nucleons, which allowed for estimates of nuclear configuration mixing [26]. The TES effect is responsible for energy anomalies in the nuclei near and especially beyond the proton drip line [27]. In our case, the $1/2^+$ g.s. of ^{29}Cl is at 1.79 MeV above the $1p$ threshold, and the excitation energy of the $3/2^+$ excited state is 0.5 MeV, which is 2.29 MeV above the $1p$ threshold. Thus, we assume that the 1.8 and 2.3 MeV peaks in Fig. 3 match the $1/2^+$ and $3/2^+$ states expected in ^{29}Cl.

Correlations in the decay of ^{30}Ar *states.*—By selecting the measured $^{28}\mathrm{S} + p + p$ data with gates on ρ_θ values corresponding to the peaks $A - H$ in Fig. 2(c), we obtain the angular $\theta(^{28}\mathrm{S}\text{-}p)$ distributions which reflect energy spectra of protons emitted from the suggested parent states in ^{30}Ar. This technique has successfully been used for revealing the structure and decay dynamics of ^{19}Mg [17]. Three such correlations gated by the lowest ρ_θ peaks A, B, and C [see Fig. 2(c)] are shown in Fig. 4. The level schemes of ^{29}Cl and ^{30}Ar, determined from a combined analysis of the distributions shown in Figs. 2(c), 3, and 4, are provided in Fig. 5.

The ^{30}Ar *g.s. assignment.*—The lowest-energy peak in the observed spectrum of ^{30}Ar [marked as A in Fig. 2(c)]

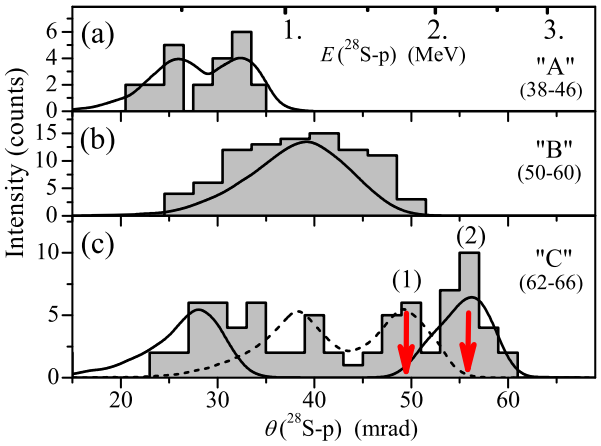

FIG. 4 (color online). The histograms (a)–(c) show angular correlations $\theta(^{28}\text{S-}p)$, which were selected from the $^{28}\text{S}+p+p$ data by using ρ_θ gates within the ranges shown under the labels A, B, and C (in mrad). The gates match the peaks in Fig. 2(c). The arrows (1,2) point to the peaks (1,2) in Fig. 3, which suggest the states in ^{29}Cl. The curves in panels: (a) Monte Carlo simulations of the detector response to a sequential $2p$ decay $^{30}\text{Ar}^*(2^+) \rightarrow {}^{29}\text{Cl}^*(3/2^+) \rightarrow {}^{28}\text{S}^*(2^+)$; (b) simulations of ^{30}Ar g.s. decaying by a true $2p$-decay mechanism [28]; (c) simulations of sequential decays $^{30}\text{Ar}^*(2^+) \rightarrow {}^{29}\text{Cl}^*(3/2^+) \rightarrow {}^{28}$S and $^{30}\text{Ar}^*(2^+) \rightarrow {}^{29}\text{Cl}^*(1/2^+) \rightarrow {}^{28}$S (solid and dashed curves, respectively).

corresponds to $E_{2p} = 1.4$ MeV. There are several arguments for why this peak cannot be assigned to the ^{30}Ar g.s. First, a consistent description of all ^{30}Ar levels and their decays is not possible in such a case. Second, the intensity of the peak is surprisingly small for a g.s. population. Previous studies of ^{16}Ne, ^{19}Mg populated in neutron-knockout reactions at intermediate energy [13,14,16] show that cross sections of the g.s. population contain a large part (of 10%–15%) of the excitation spectrum, which agrees also with studies of ^{6}Be, ^{12}O, and ^{16}Ne at lower energies [11,12,29]. Third, we rule out the 1.4 MeV g.s. assignment because of the systematics of odd-even staggering (OES) of nuclear masses, which usually shows a slow trend with the mass number [30]. The OESs of $N = 12$ isotones and of $Z = 12$ isotopes (including ^{30}Ar and its mirror nucleus ^{30}Mg) are shown in Fig. 6. The small and almost constant shift $\Delta = 0.45$ MeV observed between bound $N = 12$ and $Z = 12$ partners breaks down in the case of unbound ^{30}Ar. For instance, if we assign the ^{30}Ar g.s. 0^+ to the low-energy peak B in Fig. 2(c), then the corresponding $E_{2p} = 2.25^{+0.15}_{-0.10}$ MeV. For the $1p$-decay energy $E_p = 1.8$ MeV of the ^{29}Cl g.s., the corresponding value $E_{\text{OES}} = 1.4$ MeV is ~800 keV below the one expected from the systematic trend. However, the other known s-d shell $2p$ emitters, shown in the right part of Fig. 6, demonstrate a regular lowering of E_{OES}, and the ^{30}Ar g.s. at $E_{2p} = 2.25$ MeV fits well this trend. The alternative 1.4 MeV assignment for the ^{30}Ar g.s. [the lowest-lying peak A in Fig. 2(c)] can be clearly ruled out by these systematics: The proton spectrum from $2p$ decay of this state shown in Fig. 4(a) points to a sequential $1p$ emission with E_p of either 0.6 or 0.8 MeV. The two respective E_{OES} values are around zero, which does not match any reasonable structure of the ^{30}Ar g.s. We propose that this peak has its origin from a branch of $2p$ decay of the

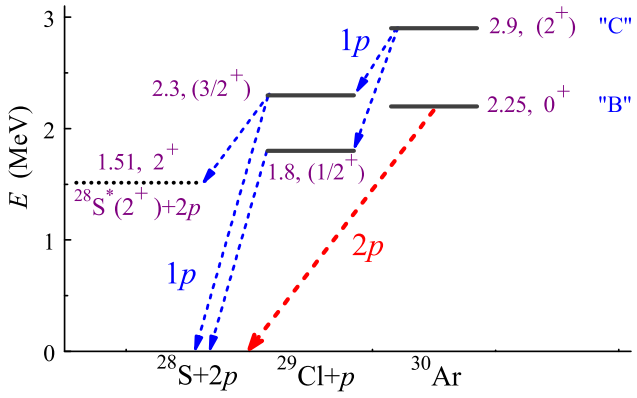

FIG. 5 (color online). Proposed decay scheme of low-lying ^{30}Ar and ^{29}Cl states, whose energy is given relative to the $2p$ and $1p$ thresholds, respectively. The assigned levels 0^+ and (2^+) in ^{30}Ar correspond to the peaks B and C in Fig. 2(c), respectively. The peak A in Fig. 2(c) comes from the $^{30}\text{Ar}^*(2^+)$ state, which decays into the excited state $^{28}\text{S}(2^+)$ by sequential $1p$ emissions via $^{29}\text{Cl}^*(3/2^+)$.

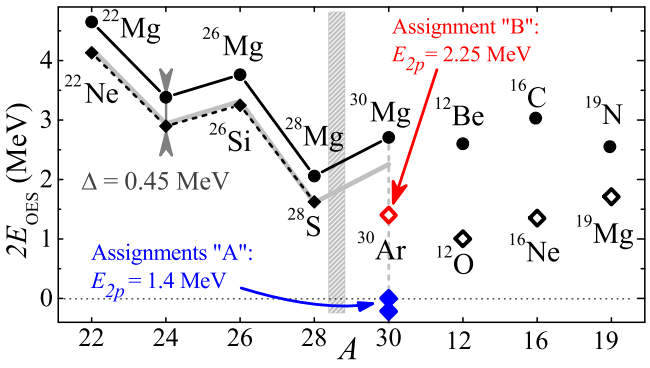

FIG. 6 (color online). Odd-even mass staggering expressed via nuclear separation energies $2E_{\text{OES}} = 2S_N - S_{2N}$ (see [30]) and applied to mirror nuclei with mass numbers A around 30. Here, S_N and S_{2N} are one-nucleon (either proton or neutron) and two-nucleon separation energies, respectively. To the left of the gray hatched bar: Data for bound $Z = 12$ nuclei and their isobaric mirrors (solid and dashed lines, respectively) exhibit a small constant shift of 0.45 MeV. The right part shows data for known s-d-shell $2p$ emitters (then $S_p = -E_p$, $S_{2p} = -E_{2p}$) and their bound mirror nuclei. The $2E_{\text{OES}}$ assignments stemming from $E_{2p}(^{30}\text{Ar})$ of 2.25 and 1.4 MeV are indicated by the red hollow and blue-filled diamonds, respectively.

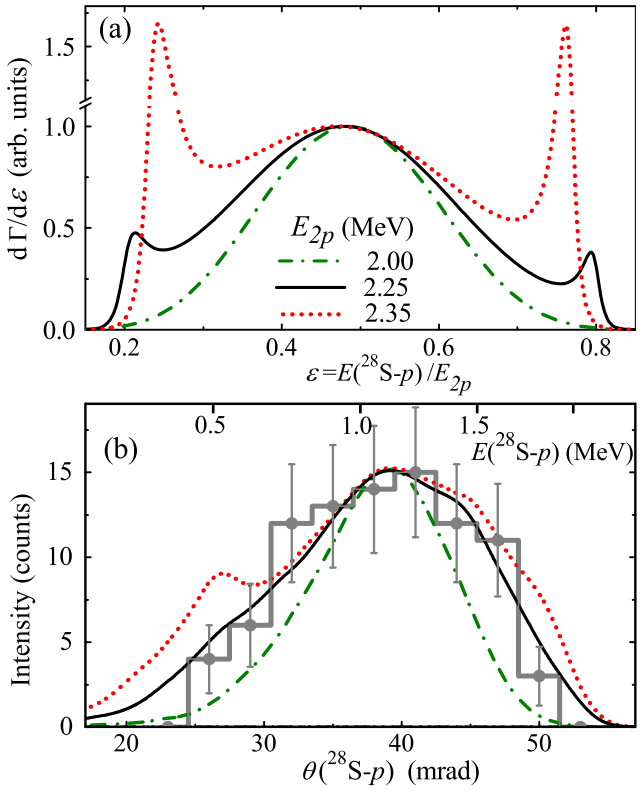

FIG. 7 (color online). Transition from the true-$2p$ decay to the sequential $1p$-emission mechanism: (a) the proton spectra calculated employing Eq. (1), where the $2p$-decay energy E_{2p} of ^{30}Ar is varied while the other parameters are fixed; (b) the respective Monte Carlo simulations of the $\theta(^{28}\text{S-}p)$ distributions compared to the data (histogram with statistical uncertainties) from Fig. 4(b).

$^{30}\text{Ar}^{*}(2^{+})$ state into the excited 2^{+} state in ^{28}S (see Fig. 5), which may represent the first case of fine structure in the $2p$ emission. An experiment that detects coincidences $^{28}\text{S}+p+p+\gamma$ with $E_{2p}=1.4$ MeV and $E_{\gamma}=1.51$ MeV might test our tentative assignment.

Decay mechanism of ^{30}Ar *g.s.*—The proton distribution from $2p$ decays of the ^{30}Ar g.s. is shown in Fig. 4(b). It is almost twice broader compared to the one predicted by a "true" $2p$ decay mechanism. Furthermore, the distribution does not point to a sequential $2p$ emission, where typical double-peak structures prevail. To solve this puzzle, we have applied a simple analytical simultaneous-emission model [4]. This model approximates well both true and sequential $2p$-decay mechanisms and yields a smooth transition between them [31,32]. The model considers protons p_i (emitted with angular momenta j_i) populating intermediate HI-p resonant states at E_{j_i}. The p-p interaction is neglected, and protons share the total decay energy E_{2p}, which is described by the parameter $\varepsilon=E(\text{HI-}p)/E_{2p}$. The $2p$-decay spectra are described by the $2p$-precursor's width,

$$\Gamma(E_{2p})=\frac{E_{2p}\langle V_3\rangle^2}{2\pi}\int_0^1 d\varepsilon\frac{\Gamma_{j_1}(\varepsilon E_{2p})}{(\varepsilon E_{2p}-E_{j_1})^2+\Gamma_{j_1}(\varepsilon E_{2p})^2/4}\times\frac{\Gamma_{j_2}[(1-\varepsilon)E_{2p}]}{[(1-\varepsilon)E_{2p}-E_{j_2}]^2+\Gamma_{j_2}[(1-\varepsilon)E_{2p}]^2/4}. \quad (1)$$

There Γ_{j_i} are the standard R-matrix expressions for $1p$-decay widths as a function of energy of the involved resonances in the $^{28}\text{S}+p_i$ subsystems. In a reasonable approximation, the matrix element $\langle V_3\rangle^2\approx(2E_{\text{OES}})^2$.

The calculations show that the ^{30}Ar decay energy is located in a transition region from the true three-body decay mechanism (characterized by a belllike spectrum centered at $\varepsilon=1/2$) and the sequential decay (with two peaks at $\varepsilon=0.75$ and at $1-\varepsilon$); see Fig. 7(a). Here the correlation pattern is extremely sensitive to calculation parameters, where small variations of E_{2p} are decisive. The respective simulations of the angular correlations in the lab system are compared with the data in Fig. 7(b). The decay of ^{30}Ar g.s. occurs exactly in an intermediate situation when two "satellite" peaks, originating from sequential decays, begin to grow on either side of the central bump, which results from true $2p$ decays. This observation is the first evidence of such an interplay of the two $2p$-decay mechanisms of a nuclear g.s. This effect is confirmed by the comparison of the ^{30}Ar half-lives predicted by the true $2p$-decay, sequential-emission, and simultaneous-emission models; see Fig. 8. The measured ^{30}Ar g.s. energy range matches the area where the half-lives by the true and sequential $2p$-decay mechanisms overlap. The estimated half-life of ^{30}Ar g.s. is 10^{-15}–10^{-16} s, which is below the measured $T_{1/2}$ limit of 10^{-11} s.

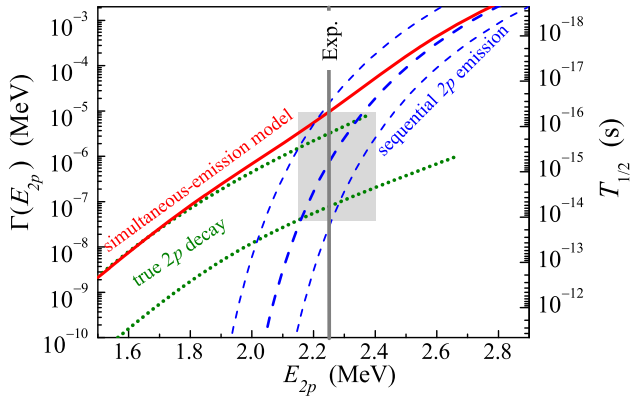

FIG. 8 (color online). Half-life of ^{30}Ar g.s. calculated with different decay mechanisms. The true $2p$-decay predictions (dotted curves) are from Ref. [28]. In sequential-emission (dashed curves) and simultaneous-emission (solid curve) models, s-wave $1p$ emission via the ^{29}Cl g.s. at $E_p=1.8\pm0.1$ MeV is assumed. The two thin dashed curves correspond to the E_p extreme values of 1.7 and 1.9 MeV. The gray box and vertical line show the $E_{2p}=2.25^{+0.15}_{-0.10}$ MeV range.

Excited states in ^{30}Ar.—Finally, we interpret the peak C in Fig. 2(c) as a (2^+) state at 2.9 MeV in ^{30}Ar decaying by two branches of sequential $1p$ emissions via the lowest states in ^{29}Cl. These assignments are based on the very different ^{28}S-p correlation patterns shown in Fig. 4(c). The tentative spin parities of the levels stem from the penetrability estimates of $1p$ emission to the respective states in ^{29}Cl. The assumed 0^+ and 2^+ states in ^{30}Ar follow the level scheme of the mirror ^{30}Mg. The peaks $D-H$ in Fig. 2(c) and 3–5 in Fig. 3 correspond to the ^{28}S-p correlations which can lead to identification of higher-excited states in ^{30}Ar and ^{29}Cl. This will be treated in forthcoming publications.

Summary.—We report the discovery of two new isotopes, ^{30}Ar and ^{29}Cl, which both are unbound. From the measured angular correlations of the decay products, a transition interplay of true three-body and sequential $2p$ decays is detected in ^{30}Ar. Such a phenomenon, never observed before, may be common in $2p$-unbound nuclei and could be of interest for other disciplines dealing with few-body systems. The indicated dramatic change of odd-even mass staggering in $2p$-unbound nuclei and the fine structure in the $2p$ decay of the ^{30}Ar*(2.9 MeV) state call for further investigations.

A. G., S. K., S. R., and P. S. were supported by the Helmholtz Association Grant No. IK-RU-002. L. V. G. was partly supported by the Ministry of Education and Science of the Russian Federation Grant No. NSh-932.2014.2. A. F., A. G., L. V. G., S. K., P. S., and R. S. were partly supported by the Russian Foundation for Basic Research Grant No. 14-02-00090-a. This work was partly supported by the Polish National Science Center under Contract No. UMO-2011/01/B/ST2/01943. A. A. C. acknowledges support by the Polish Ministry of Science and Higher Education by Grant No. 0079/DIA/2014/43 (Grant Diamentowy). M. P. and X. X. are grateful for a support from the Helmholtz International Center for FAIR (HIC for FAIR). Y. L. was supported by the Helmholtz-CAS Joint Research Group Grant No. HCJRG-108. J. M. E. acknowledges support from the FPA2009-08848 contract (MICINN, Spain). Authors declare that this article is a part of PhD thesis of X. X.

[1] M. Pfützner, E. Badura, C. Bingham, B. Blank, M. Chartier, H. Geissel, J. Giovinazzo, L. V. Grigorenko, R. Grzywacz, M. Hellström, Z. Janas, J. Kurcewicz, A. S. Lalleman, C. Mazzocchi, I. Mukha, G. Münzenberg, C. Plettner, E. Roeckl, K. P. Rykaczewski, K. Schmidt, R. S. Simon, M. Stanoiu, and J. C. Thomas, Eur. Phys. J. A **14**, 279 (2002).

[2] J. Giovinazzo, B. Blank, M. Chartier, S. Czajkowski, A. Fleury, M. J. L. Jimenez, M. S. Pravikoff, J. C. Thomas, F. de Oliveira Santos, M. Lewitowicz, V. Maslov, M. Stanoiu, R. Grzywacz, M. Pfützner, C. Borcea, and B. A. Brown, Phys. Rev. Lett. **89**, 102501 (2002).

[3] V. I. Goldansky, Nucl. Phys. **19**, 482 (1960).

[4] M. Pfützner, M. Karny, L. V. Grigorenko, and K. Riisager, Rev. Mod. Phys. **84**, 567 (2012).

[5] B. Blank, A. Bey, G. Canchel, C. Dossat, A. Fleury, J. Giovinazzo, I. Matea, N. Adimi, F. De Oliveira, I. Stefan, G. Georgiev, S. Grevy, J. C. Thomas, C. Borcea, D. Cortina, M. Caamano, M. Stanoiu, F. Aksouh, B. A. Brown, F. C. Barker, and W. A. Richter, Phys. Rev. Lett. **94**, 232501 (2005).

[6] M. Pomorski, M. Pfützner, W. Dominik, R. Grzywacz, T. Baumann, J. S. Berryman, H. Czyrkowski, R. Dabrowski, T. Ginter, J. Johnson, G. Kamiński, A. Kuźniak, N. Larson, S. N. Liddick, M. Madurga, C. Mazzocchi, S. Mianowski, K. Miernik, D. Miller, S. Paulauskas, J. Pereira, K. P. Rykaczewski, A. Stolz, and S. Suchyta, Phys. Rev. C **83**, 061303 (2011).

[7] K. Miernik, W. Dominik, Z. Janas, M. Pfützner, L. Grigorenko, C. R. Bingham, H. Czyrkowski, M. Cwiok, I. G. Darby, R. Dabrowski, T. Ginter, R. Grzywacz, M. Karny, A. Korgul, W. Kusmierz, S. N. Liddick, M. Rajabali, K. Rykaczewski, and A. Stolz, Phys. Rev. Lett. **99**, 192501 (2007).

[8] P. Ascher, L. Audirac, N. Adimi, B. Blank, C. Borcea, B. A. Brown, I. Companis, F. Delalee, C. E. Demonchy, F. de Oliveira Santos, J. Giovinazzo, S. Grévy, L. V. Grigorenko, T. Kurtukian-Nieto, S. Leblanc, J.-L. Pedroza, L. Perrot, J. Pibernat, L. Serani, P. C. Srivastava, and J.-C. Thomas, Phys. Rev. Lett. **107**, 102502 (2011).

[9] M. Pomorski, M. Pfützner, W. Dominik, R. Grzywacz, A. Stolz, T. Baumann, J. S. Berryman, H. Czyrkowski, R. Dąbrowski, A. Fijałkowska, T. Ginter, J. Johnson, G. Kamiński, N. Larson, S. N. Liddick, M. Madurga, C. Mazzocchi, S. Mianowski, K. Miernik, D. Miller, S. Paulauskas, J. Pereira, K. P. Rykaczewski, and S. Suchyta, Phys. Rev. C **90**, 014311 (2014).

[10] A. Fomichev, V. Chudoba, I. Egorova, S. Ershov, M. Golovkov, A. Gorshkov, V. Gorshkov, L. Grigorenko, G. Kamiski, S. Krupko, I. Mukha, Y. Parfenova, S. Sidorchuk, R. Slepnev, L. Standyo, S. Stepantsov, G. Ter-Akopian, R. Wolski, and M. Zhukov, Phys. Lett. B **708**, 6 (2012).

[11] I. A. Egorova, R. J. Charity, L. V. Grigorenko, Z. Chajecki, D. Coupland, J. M. Elson, T. K. Ghosh, M. E. Howard, H. Iwasaki, M. Kilburn, J. Lee, W. G. Lynch, J. Manfredi, S. T. Marley, A. Sanetullaev, R. Shane, D. V. Shetty, L. G. Sobotka, M. B. Tsang, J. Winkelbauer, A. H. Wuosmaa, M. Youngs, and M. V. Zhukov, Phys. Rev. Lett. **109**, 202502 (2012).

[12] K. W. Brown, R. J. Charity, L. G. Sobotka, Z. Chajecki, L. V. Grigorenko, I. A. Egorova, Y. L. Parfenova, M. V. Zhukov, S. Bedoor, W. W. Buhro, J. M. Elson, W. G. Lynch, J. Manfredi, D. G. McNeel, W. Reviol, R. Shane, R. H. Showalter, M. B. Tsang, J. R. Winkelbauer, and A. H. Wuosmaa, Phys. Rev. Lett. **113**, 232501 (2014).

[13] I. Mukha, K. Sümmerer, L. Acosta, M. A. G. Alvarez, E. Casarejos, A. Chatillon, L. Cortina-Gil, J. Espino, A. Fomichev, J. E. Garcia-Ramos, H. Geissel, J. Gomez-Camacho, L. Grigorenko, J. Hofmann, O. Kiselev, A. Korsheninnikov, N. Kurz, Y. Litvinov, I. Martel, C. Nociforo, W. Ott, M. Pfützner, C. Rodriguez-Tajes, E. Roeckl, M. Stanoiu, H. Weick, and P. J. Woods, Phys. Rev. Lett. **99**, 182501 (2007).

[14] I. Mukha, L. Grigorenko, K. Sümmerer, L. Acosta, M. A. G. Alvarez, E. Casarejos, A. Chatillon, D. Cortina-Gil, J. M. Espino, A. Fomichev, J. E. García-Ramos, H. Geissel, J. Gómez-Camacho, J. Hofmann, O. Kiselev, A. Korsheninnikov, N. Kurz, Y. Litvinov, I. Martel, C. Nociforo, W. Ott, M. Pfützner, C. Rodríguez-Tajes, E. Roeckl, M. Stanoiu, H. Weick, and P. J. Woods, Phys. Rev. C **77**, 061303 (2008).

[15] I. Mukha, N. K. Timofeyuk, K. Sümmerer, L. Acosta, M. A. G. Alvarez, E. Casarejos, A. Chatillon, D. Cortina-Gil, J. M. Espino, A. Fomichev, J. E. García-Ramos, H. Geissel, J. Gómez-Camacho, L. Grigorenko, J. Hofmann, O. Kiselev, A. Korsheninnikov, N. Kurz, Y. Litvinov, I. Martel, C. Nociforo, W. Ott, M. Pfützner, C. Rodríguez-Tajes, E. Roeckl, M. Stanoiu, H. Weick, and P. J. Woods, Phys. Rev. C **79**, 061301 (2009).

[16] I. Mukha, K. Sümmerer, L. Acosta, M. A. G. Alvarez, E. Casarejos, A. Chatillon, D. Cortina-Gil, I. A. Egorova, J. M. Espino, A. Fomichev, J. E. García-Ramos, H. Geissel, J. Gómez-Camacho, L. Grigorenko, J. Hofmann, O. Kiselev, A. Korsheninnikov, N. Kurz, Y. A. Litvinov, E. Litvinova, I. Martel, C. Nociforo, W. Ott, M. Pfützner, C. Rodríguez-Tajes, E. Roeckl, M. Stanoiu, N. K. Timofeyuk, H. Weick, and P. J. Woods, Phys. Rev. C **82**, 054315 (2010).

[17] I. Mukha, L. Grigorenko, L. Acosta, M. A. G. Alvarez, E. Casarejos, A. Chatillon, D. Cortina-Gil, J. M. Espino, A. Fomichev, J. E. García-Ramos, H. Geissel, J. Gómez-Camacho, J. Hofmann, O. Kiselev, A. Korsheninnikov, N. Kurz, Y. A. Litvinov, I. Martel, C. Nociforo, W. Ott, M. Pfützner, C. Rodríguez-Tajes, E. Roeckl, C. Scheidenberger, M. Stanoiu, K. Sümmerer, H. Weick, and P. J. Woods, Phys. Rev. C **85**, 044325 (2012).

[18] H. Geissel, P. Armbruster, K. Behr, A. Bruenle, K. Burkard, M. Chen, H. Folger, B. Franczak, H. Keller, O. Klepper, B. Langenbeck, F. Nickel, E. Pfeng, M. Pfuetzner, E. Roeckl, K. Rykaczewski, I. Schall, D. Schardt, C. Scheidenberger, K.-H. Schmidt, A. Schroeter, T. Schwab, K. Suemmerer, M. Weber, G. Muenzenberg, T. Brohm, H.-G. Clerc, M. Fauerbach, J.-J. Gaimard, A. Grewe, E. Hanelt, B. Knoedler, M. Steiner, B. Voss, J. Weckenmann, C. Ziegler, A. Magel, H. Wollnik, J. Dufour, Y. Fujita, D. Vieira, and B. Sherrill, Nucl. Instrum. Methods Phys. Res., Sect. B **70**, 286 (1992).

[19] A. A. Lis, C. Mazzocchi, W. Dominik, Z. Janas, M. Pfützner, M. Pomorski, L. Acosta, S. Baraeva, E. Casarejos, J. Duénas-Díaz, V. Dunin, J. M. Espino, A. Estrade, F. Farinon, A. Fomichev, H. Geissel, A. Gorshkov, G. Kamiński, O. Kiselev, R. Knöbel, S. Krupko, M. Kuich, Y. A. Litvinov, G. Marquinez-Durán, I. Martel, I. Mukha, C. Nociforo, A. K. Ordúz, S. Pietri, A. Prochazka, A. M. Sánchez-Benítez, H. Simon, B. Sitar, R. Slepnev, M. Stanoiu, P. Strmen, I. Szarka, M. Takechi, Y. Tanaka, H. Weick, and J. S. Winfield, Phys. Rev. C **91**, 064309 (2015).

[20] P. Voss, T. Baumann, D. Bazin, A. Dewald, H. Iwasaki, D. Miller, A. Ratkiewicz, A. Spyrou, K. Starosta, M. Thoennessen, C. Vaman, and J. A. Tostevin, Phys. Rev. C **90**, 014301 (2014).

[21] S. Agostinelli, J. Allison, K. Amako, J. Apostolakis, H. Araujo, P. Arce, M. Asai, D. Axen, S. Banerjee, G. Barrand, F. Behner, L. Bellagamba, J. Boudreau, L. Broglia, A. Brunengo, H. Burkhardt, S. Chauvie, J. Chuma, R. Chytracek, G. Cooperman, G. Cosmo, P. Degtyarenko, A. Dell'Acqua, G. Depaola, D. Dietrich, R. Enami, A. Feliciello, C. Ferguson, H. Fesefeldt, G. Folger, F. Foppiano, A. Forti, S. Garelli, S. Giani, R. Giannitrapani, D. Gibin, J. G. Cadenas, I. González, G. G. Abril, G. Greeniaus, W. Greiner, V. Grichine, A. Grossheim, S. Guatelli, P. Gumplinger, R. Hamatsu, K. Hashimoto, H. Hasui, A. Heikkinen, A. Howard, V. Ivanchenko, A. Johnson, F. Jones, J. Kallenbach, N. Kanaya, M. Kawabata, Y. Kawabata, M. Kawaguti, S. Kelner, P. Kent, A. Kimura, T. Kodama, R. Kokoulin, M. Kossov, H. Kurashige, E. Lamanna, T. Lampén, V. Lara, V. Lefebure, F. Lei, M. Liendl, W. Lockman, F. Longo, S. Magni, M. Maire, E. Medernach, K. Minamimoto, P. M. de Freitas, Y. Morita, K. Murakami, M. Nagamatu, R. Nartallo, P. Nieminen, T. Nishimura, K. Ohtsubo, M. Okamura, S. O'Neale, Y. Oohata, K. Paech, J. Perl, A. Pfeiffer, M. Pia, F. Ranjard, A. Rybin, S. Sadilov, E. D. Salvo, G. Santin, T. Sasaki, N. Savvas, Y. Sawada, S. Scherer, S. Sei, V. Sirotenko, D. Smith, N. Starkov, H. Stoecker, J. Sulkimo, M. Takahata, S. Tanaka, E. Tcherniaev, E. S. Tehrani, M. Tropeano, P. Truscott, H. Uno, L. Urban, P. Urban, M. Verderi, A. Walkden, W. Wander, H. Weber, J. Wellisch, T. Wenaus, D. Williams, D. Wright, T. Yamada, H. Yoshida, and D. Zschiesche, Nucl. Instrum. Methods Phys. Res., Sect. A **506**, 250 (2003).

[22] P. Baumann, P. Dessagne, A. Huck, G. Klotz, A. Knipper, G. Marguier, C. Miehé, M. Ramdane, C. Richard-Serre, G. Walter, and B. H. Wildenthal, Phys. Rev. C **36**, 765 (1987).

[23] I. Angeli and K. Marinova, At. Data Nucl. Data Tables **99**, 69 (2013).

[24] R. G. Thomas, Phys. Rev. **88**, 1109 (1952).

[25] J. B. Ehrman, Phys. Rev. **81**, 412 (1951).

[26] L. V. Grigorenko, T. A. Golubkova, and M. V. Zhukov, Phys. Rev. C **91**, 024325 (2015).

[27] E. Comay, I. Kelson, and A. Zidon, Phys. Lett. B **210**, 31 (1988).

[28] L. V. Grigorenko, I. G. Mukha, and M. V. Zhukov, Nucl. Phys. **A714**, 425 (2003); **740**, 401(E) (2004).

[29] M. F. Jager, R. J. Charity, J. M. Elson, J. Manfredi, M. H. Mahzoon, L. G. Sobotka, M. McCleskey, R. G. Pizzone, B. T. Roeder, A. Spiridon, E. Simmons, L. Trache, and M. Kurokawa, Phys. Rev. C **86**, 011304 (2012).

[30] W. Friedman and G. Bertsch, Eur. Phys. J. A **41**, 109 (2009).

[31] L. V. Grigorenko and M. V. Zhukov, Phys. Rev. C **76**, 014008 (2007).

[32] L. V. Grigorenko and M. V. Zhukov, Phys. Rev. C **76**, 014009 (2007).